NANO LETTERS

2007
Vol. 7, No. 10
2981−2986

Fluorescence Probes for Membrane Potentials Based on Mesoscopic Electron Transfer

Liang-shi Li†

Department of Chemistry, Indiana University, Bloomington Indiana 47405

Received May 17, 2007; Revised Manuscript Received July 24, 2007

ABSTRACT

A new type of voltage-sensitive dye is proposed based on the electric-field dependence of electron transfer. These dyes contain an electron donor–acceptor pair in which intramolecular electron transfer competes with fluorescence emission, converting changes in electric field to those in fluorescence intensity. With electron-transfer distance of nanometers, theoretical analysis shows that these dyes can have high sensitivity to neuron action potentials with high fluorescence quantum yield, allowing for fast optical neuroimaging with large signal-to-noise ratio.

Understanding how electrical signals propagate within single neurons and among ensembles of neurons is key to elucidating mechanisms of information processing in the central nervous system. Optical imaging techniques have the advantage of allowing many locations to be simultaneously and noninvasively monitored with high spatial and temporal resolution[1−5] and therefore are preferred for measuring activity of neurons in their social context. Existing voltage-sensitive optical probes or dyes that are fast enough to track neuronal signals, however, suffer from low signal-to-noise ratio[1,6,7] and varying voltage responses from species to species[6,8] and therefore have limited uses in neuronal imaging. This is partly because the highly voltage-responsive signals in their absorption or fluorescence usually have low amplitudes[9,10] and partly because their voltage response mechanisms are environment dependent.[6,8] Thus, it is desirable to develop new voltage-sensitive dyes with a universal voltage response mechanism, high voltage sensitivity, large fluorescence intensities, and fast time responses. In this letter, I propose a new mechanism to measure membrane potentials using the electric-field dependence of electron transfer.[11−13] Calculations based on Marcus theory[14−16] show that with properly selected electron donor−acceptor pairs, this mechanism may lead to a new class of voltage-sensitive dyes for measuring membrane potentials with both large signal-to-noise ratios and fast time responses.

Action potentials are of central importance to interneuronal communication.[17] At rest, neurons maintain a resting potential of about −70 mV relative to the outside of the cells. Under stimuli of sufficient amplitudes, the potential inside a cell reaches a peak value of about +30 mV within a millisecond.[17] Therefore, effective voltage-sensitive dyes should have sufficient sensitivity to convert the change in electric field from −14 to +6 mV/nm (or −140 to +60 kV/cm) across the membrane (membrane thickness taken as 5 nm)[18] to a detectable optical signal, preferably with a submillisecond response time and a large signal-to-noise ratio.

Electron transfer between electron donors and acceptors is electric-field dependent[11,12] and therefore in principle can be used to measure electric fields. In addition, photoassisted electron transfer often efficiently competes with fluorescence emission, leading to partial or complete fluorescence quenching.[13,19−22] As a result, by measuring the change in fluorescence quantum yield from an electron donor−acceptor system under an external electric field, we can determine the change in the electric field. For the purpose of developing new fluorescence probes for membrane potentials, we consider amphiphilic compounds containing a donor−acceptor pair separated by a spacer (Figure 1a). The amphiphilicity of the compounds is necessary for incorporating the compounds in membrane bilayers and aligning them relative to the electric fields. The donor and acceptor chromophores chosen here have properly aligned energy levels for the highest occupied molecular orbitals (HOMOs) and the lowest unoccupied molecular orbitals (LUMOs), favoring electron transfer when either the donor or the acceptor is photoexcited (Figure 1b,c). The spacer, on the other hand, defines the distance of electron transfer, which, as shown later in this manuscript, largely determines the sensitivity of voltage measurements.

The electronic structure of donor−acceptor pair can be alternatively represented by a three-level diagram (Figure 1d), and the competition between the electron transfer and the fluorescence emission can be solved analytically. In Figure 1d, state 1 represents the fluorescence-emitting state,

† E-mail: li23@indiana.edu.

10.1021/nl071163p CCC: $37.00
Published on Web 09/20/2007

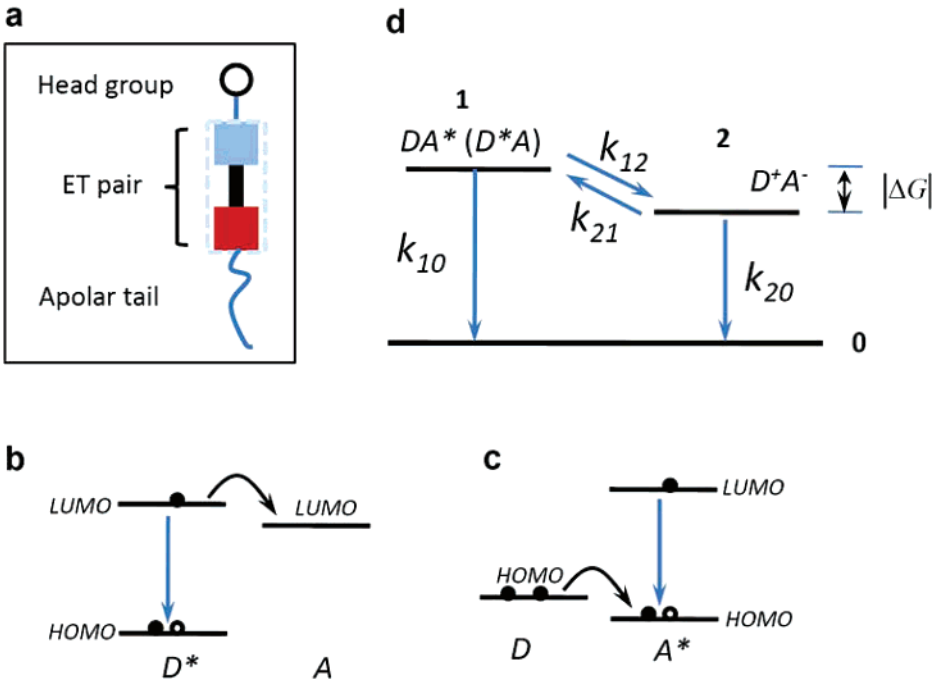

Figure 1. (a) Schematic representation of an amphiphilic molecule containing an electron-transfer (ET) pair. (b,c) The energy levels of the donor (D) and the acceptor (A). The fluorescence emitters are labeled with an asterisk, which are the donor in (b) and the acceptor in (c), respectively. The blue arrows indicate fluorescence generation, and the black arrows denote electron transfer, which quenches the fluorescence. (d) The energy levels of the donor−acceptor pair, with the arrows indicating possible transition pathways between the energy levels. The k values are the rate constants for these transitions.

2 the charge-separated state, and 0 the ground state. ΔG is the free energy change when an electron transfers from state 1 to state 2. The k values are the rate constants of the transitions between the states involved, among which $k_{10} = k_f + k_{NR}$ is the summation of the radiative relaxation rate constant k_f and the nonradiative relaxation rate constant k_{NR}. Typically k_f ranges from 10^5 to 10^9 s^{-1} [23] and k_{12} from 10^5 to 10^{12} s^{-1}.[24] With this simple model, we can solve for the population density of states 1 and 2 with kinetic equations

$$\frac{d}{dt}P_1(t) = -(k_{10} + k_{12})P_1(t) + k_{21}P_2(t)$$

$$\frac{d}{dt}P_2(t) = -(k_{20} + k_{21})P_2(t) + k_{12}P_1(t)$$

With state 1 populated by photoexcitation, we have the initial condition $P_1(t = 0) = 1$ and $P_2(t = 0) = 0$ and obtain:

$$P_1(t) = \frac{k_2 + K_1}{K_1 - K_2} e^{K_1 t} - \frac{k_2 + K_2}{K_1 - K_2} e^{K_2 t}$$

$$P_2(t) = \frac{k_{12}}{K_1 - K_2}(e^{K_1 t} - e^{K_2 t})$$

where

$$K_{1,2} = -\frac{1}{2}(k_1 + k_2) \pm \frac{1}{2}\sqrt{(k_1 - k_2)^2 + 4k_{12}k_{21}}$$

and $k_1 = k_{10} + k_{12}$, $k_2 = k_{20} + k_{21}$

Fluorescence quantum yield of state 1 is calculated as

$$Y_f = k_f \int_0^\infty dt\, P_1(t) = \frac{k_f \cdot k_2}{K_1 K_2} = \frac{k_f \cdot (k_{21} + k_{20})}{(k_{10} + k_{12})(k_{21} + k_{20}) - k_{12}k_{21}} \quad (1)$$

which is sensitive to external electric fields because the latter can considerably alter k_{12}, k_{21}, and k_{20}. In this letter, we assume the energy levels and other photophysical properties of the neutral donor and acceptor chromophores, such as k_{10}, k_f, their absorption spectra, and their fluorescence spectra, to be unaffected by the electric fields because the electric fields affect neutral molecules much less significantly than they do to the electron-transfer products, i.e., donor−acceptor ion pairs.

With the Marcus−Levich−Jortner's formulism,[13,15] we can calculate the value of electron-transfer rate constant k_{12},

$$k_{12} = V^2 \left(\frac{4\pi^2}{h}\right)\left(\frac{1}{4\pi\lambda_m k_B T}\right)^{1/2} e^{-S_c}\left\{\sum_{n=0}^{+\infty}\frac{S_c^n}{n!} \exp\left[-\frac{(\Delta G + \lambda_m + nh\omega_c)^2}{4\lambda_m k_B T}\right]\right\}$$

$$= A \times \left\{\sum_{n=0}^{+\infty}\frac{S_c^n}{n!}\exp\left[-\frac{(\Delta G + \lambda_m + nh\omega_c)^2}{4\lambda_m k_B T}\right]\right\} \quad (2)$$

k_{21} can be calculated with the detailed balance relation

$$k_{21} = k_{12}\, e^{\Delta G/k_B T} \tag{3}$$

Here V is the electronic coupling constant between state 1 and 2, λ_m the reorganization energy of the surrounding medium, ω_c the average frequency of the high-frequency intramolecular vibrational modes that facilitate the electron-transfer process, and S_c the electron−phonon coupling strength of these modes.[13,15] k_B and h are Boltzmann's and Planck's constants, respectively. The free energy change ΔG during electron transfer can be altered by an external electric field following

$$\Delta G = \Delta G_0 - \Delta\vec{\mu}\cdot\vec{E} \tag{4}$$

with ΔG_0 being the free energy change under zero field and $\Delta\vec{\mu}$ the change in the electric dipole moment of the donor−acceptor pair when the electron transfer occurs (its magnitude approximately proportional to the donor−acceptor distance). For electron transfer over a mesoscopic distance whose upper limit is set by the membrane thickness (~5 nm), the field effect on electron transfer can be quite significant, leading to a considerable change in the electron-transfer rates and therefore the fluorescence quantum yield of the donor−acceptor pair. Here we use the fractional change in fluorescence quantum yield when the transmembrane electric fields change from −14 to +6 mV/nm (corresponding to a 100 mV change in membrane potentials) to represent the voltage sensitivity of the dyes.

Figure 2 shows the normalized electron-transfer rate k_{12}/A (A defined in eq 2) calculated with eq 2 as a function of ΔG at 310 K. The maximal value at −100 meV and the shoulders at −280 and −500 meV correspond to $\Delta G + \lambda_m + nh\omega_c \approx 0$, where $n = 0$, 1, and 2, respectively. Obviously, fluorescence from electron-transfer systems with ΔG falling in the regions with large slopes (i.e., $\Delta G \sim 0$, −180, −360, and −560 meV) are more sensitive toward membrane potential changes. Naturally, a larger dipole moment change leads to a greater variation of ΔG with a given change in external electric fields, and therefore electron transfer over a mesoscopic distance is desired for high voltage sensitivity. For all the calculations in this letter, the parameters adopted are $\lambda_m = 800\ cm^{-1}$, $\omega_c = 1500\ cm^{-1}$, and $S_c = 0.5$, following the accepted values for the primary electron-transfer process in photosynthetic reaction centers.[13] This is a reasonable estimation because both voltage-sensitive dyes and photosynthetic reaction centers locate in a similar environment (cell membranes) and both involve conjugated chromophores.

A particularly simple case is when $\Delta G < 0$, with its absolute value much larger than the thermal energy $k_B T$. The large free energy change upon electron-transfer stabilizes state 2 and virtually eliminates k_{21} (see eq 3). The fluorescence quantum yield (eq 1) can now be simplified as

$$Y_f = \frac{k_f}{k_{10} + k_{12}} = \frac{k_f}{k_{10}} \cdot \frac{k_{10}}{k_{10} + k_{12}} = Y_{f0}\left(\frac{1}{1 + k_{12}/k_{10}}\right) \tag{5}$$

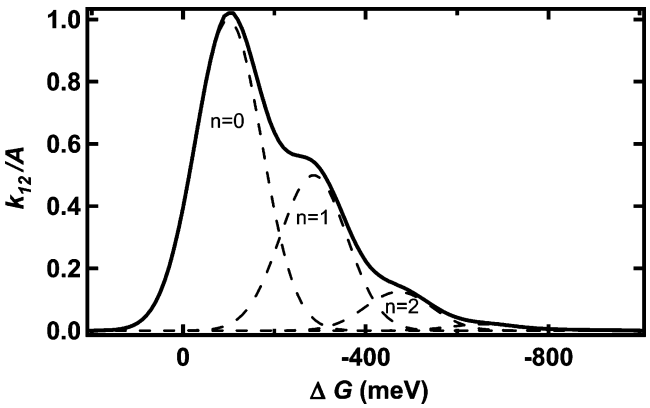

Figure 2. Normalized electron-transfer rate k_{12}/A at 310 K (solid curve) as a function of the electron-transfer free energy ΔG defined in Figure 1d. The parameters used for the calculation are described in the text. Also shown as the dashed curves are the contributions from the first three terms in eq 2, whose peak values correspond to $\Delta G + \lambda_m + nh\omega_c = 0$, with $n = 0$, 1, and 2, respectively.

where Y_{f0} is the fluorescence quantum yield of the emitting chromophore (donor in Figure 1b and acceptor in Figure 1c) when there is no electron transfer occurring (i.e., $k_{12} = 0$).

To demonstrate the voltage sensitivity of the fluorescence from the donor−acceptor pair, we consider a system with ΔG_0 falling within one of the regions in Figure 2 with large slopes. The fluorescence quantum yield Y_f (normalized with respect to Y_{f0}) at 310 K as a function of the external electric field is plotted in Figure 3a. Here, the electron-transfer process has $\Delta G_0 = -360$ meV and a moderate dipole moment change $|\Delta\vec{\mu}| = 60$ Debye (corresponding to an electron-transfer distance of 1.25 nm). In Figure 3a, the electric-field dependence of fluorescence quantum yield is shown for electron transfer of different rates symbolized by various $k_{12}^{(0)}/k_{10}$ values, with $k_{12}^{(0)}$ representing the electron-transfer rate k_{12} under zero electric field. The curves, resembling the one in Figure 2 inverted, also have shoulders and regions of large slopes. Under the same electric field, donor−acceptor pairs with faster electron transfer (larger values of $k_{12}^{(0)}/k_{10}$) have smaller fluorescence quantum yield, for electron-transfer quenches fluorescence. Here the direction of electron transfer is assumed to be such that a positive field stabilizes the electron-transfer product (i.e., ΔG more negative), reduces the electron-transfer rate (ΔG is in "inverted region"), and therefore increases the fluorescence quantum yield. This in practice can be achieved by loading the amphiphilic molecules into the outer leaflet of membrane bilayers. The field dependence of parameters V, λ_m, ω_c, S_c, and $\Delta\vec{\mu}$ is neglected because electric fields modify them much less significantly.

To appreciate how much the fluorescence quantum yield changes as the membrane potential changes from the resting potential of −14 mV/nm (red vertical line in Figure 3a) to the peak potential of 6 mV/nm (blue vertical line in Figure 3a), we plot in Figure 3b the normalized fluorescence quantum yield Y_f/Y_{f0} under the two potentials (red and blue curves, respectively, left axis) as a function of electron-transfer rate $k_{12}^{(0)}/k_{10}$. Same as in Figure 3a, the increasing electron-transfer rate decreases the fluorescence quantum

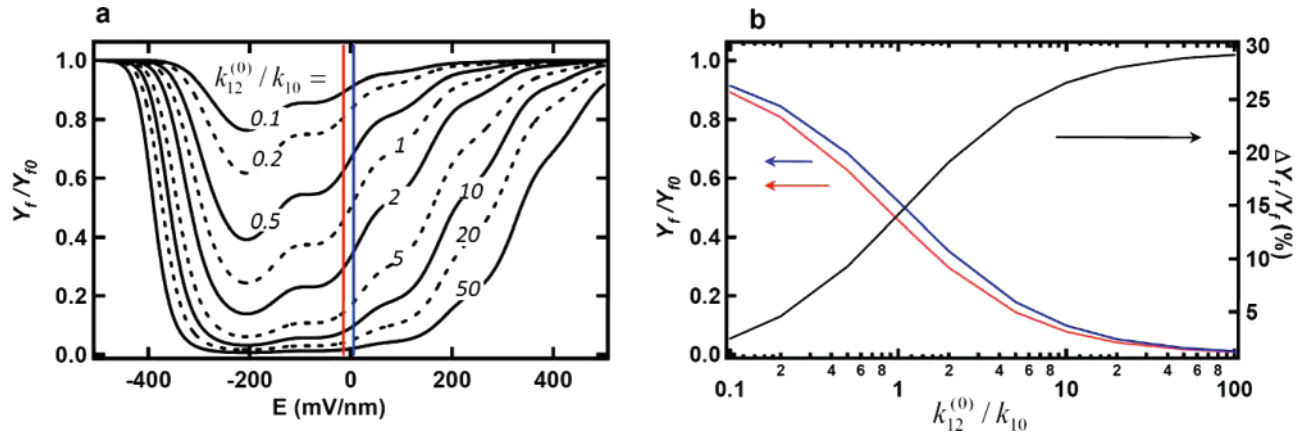

Figure 3. (a) Normalized fluorescence quantum yield Y_f/Y_{f0} as functions of the electric field for an electron-transfer process with $\Delta G_0 = -360$ meV and dipole-moment change $|\Delta\vec{\mu}| = 60$ Debye. Different curves are for different $k_{12}^{(0)}/k_{10}$ values, with $k_{12}^{(0)}$ being the zero-field value of the electron-transfer rate k_{12}. The vertical red and blue lines represent the resting and peak membrane potentials (−14 and 6 mV/nm), respectively, during neuronal activities. (b) Left axis, normalized fluorescence quantum yield Y_f/Y_{f0} under an electric field of −14 mV/nm (red curve) and 6 mV/nm (blue curve) as functions of $k_{12}^{(0)}/k_{10}$. Right axis, the fractional change in the fluorescence quantum yield, i.e., the voltage sensitivity $\Delta Y_f/Y_f$ as a function of $k_{12}^{(0)}/k_{10}$. The temperature for both figures is 310 K.

efficiency. The voltage sensitivity, represented by the fractional change, $\Delta Y_f/Y_f$, in the fluorescence quantum yield under these two potentials, is also shown (black curve, right axis), with the denominator Y_f being the initial fluorescence quantum yield (i.e., under the resting potential). Contrary to the fluorescence quantum yield, voltage sensitivity increases with increasing electron-transfer rate. Therefore, there exists a compromise between voltage sensitivity and fluorescence quantum yield, with larger voltage sensitivity $\Delta Y_f/Y_f$ corresponding to an electron-transfer rate that lowers fluorescence quantum yield Y_f/Y_{f0}. However, a range of $k_{12}^{(0)}/k_{10}$ values that yield reasonably large values for both quantities can be identified from Figure 3b. For example, a voltage sensitivity $\Delta Y_f/Y_f$ of 22% can be achieved with a fluorescence quantum yield of 0.3 (assuming $Y_{f0} = 1$, i.e., $k_f = k_{10}$). Such voltage sensitivity is already comparable to the highest values for currently existing fast voltage-sensitive dyes.[10] If an electron-transfer pair with a larger dipole moment change (than 60 Debye) is chosen, the voltage sensitivity can be further enhanced. In addition, because the voltage sensitivity $\Delta Y_f/Y_f$ describes the change in fluorescence quantum yield, it allows all the emitted photons to be collected for the detection of membrane voltage changes. This is drastically different from the existing fluorescent voltage-sensitive dyes in which large voltage sensitivity occurs only near the edges of the fluorescence spectra.[10] Therefore, together with the high-fluorescence quantum yield, the fluorescence probes based on electron transfer can lead to photon counts in optical measurements hundreds of times larger and increase the often shot-noise-limited signal-to-noise ratio by more than 1 order of magnitude.[1,7] Because of the typical rates of electron transfer (10^5−10^{12} s^{-1}) and fluorescence emission (10^5−10^9 s^{-1}), the response time of this type of fluorescence probes can easily be in the submicrosecond range.

The electron-transfer distance is a key parameter controlling the voltage response of fluorescence, and its inhomogeneity may significantly affect the voltage sensitivity. The electron-transfer distance d not only determines the change

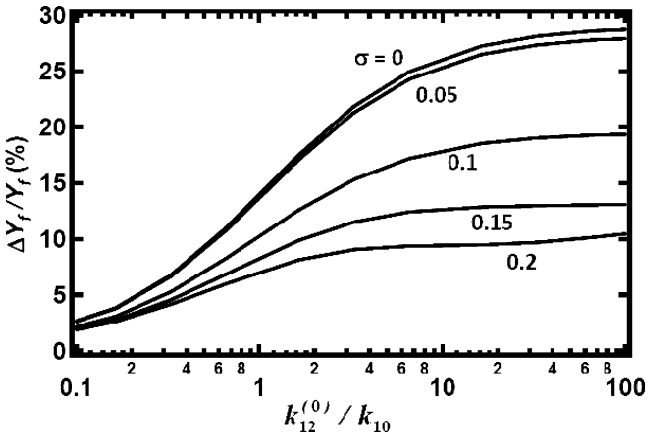

Figure 4. Voltage sensitivity $\Delta Y_f/Y_f$ decreases as a result of inhomogeneity in the donor−acceptor distance d. The distance d is assumed to follow a Gaussian-like distribution $P(d) = C \exp\{-(d - d_0)^2/\sigma^2 d_0^2\}$, $d > 0$ where $d_0 = 1.25$ nm, and C is the normalization constant. The x-axis is the zero-field electron-transfer rate with $d = d_0$, the most probable value. Different curves are for different σ values.

in the dipole moment $\Delta\vec{\mu}$ but also the zero-field free energy change[25] ΔG_0, electronic coupling constant[26] V, and the reorganization energy λ_m. For a given donor−acceptor pair, $\Delta\vec{\mu}$ is approximately proportional to d, ΔG_0 is distance-dependent[25] through Columbic interaction $-e^2/\epsilon d$, V is proportional to $\exp(-d/2R_0)$,[26] and the distance-dependence of λ_m can be evaluated with the classical dielectric continuum model developed by Marcus.[14,16] Here ϵ is the dielectric constant of the surrounding media and R_0 the characteristic distance depending on the chemical nature of the spacer.[26] Knowing these relations, we can evaluate the effect of inhomogeneity in d on the voltage sensitivity.

Figure 4 shows the dependence of the voltage sensitivity on electron-transfer rate, with d following a Gaussian-like distribution centered at 1.25 nm with different widths σ. The distribution of the electron-transfer distance d is assumed to follow $P(d) = C \exp\{-(d - d_0)^2/\sigma^2 d_0^2\}$, where $d > 0$, $d_0 =$

1.25 nm, and C is the normalization constant. The overall voltage sensitivity is calculated by averaging over the various electron-transfer distances: $\langle \Delta Y_f/Y_f \rangle_{avg} = \int_0^{+\infty} ds\ [P(s)\Delta Y_f(s)]/\int_0^{+\infty} ds\ [P(s)Y_f(s)]$, where $Y_f(s)$ is the fluorescence quantum yield of the dyes with an electron-transfer distance of s under the resting neuronal potential. The curve for $\sigma = 0$ is identical to the one in Figure 3b. However, with increasing σ, the voltage sensitivity is significantly reduced, suggesting that rigid spacers should be preferred between the electron donor−acceptor pair for maximal voltage sensitivity. For this calculation, the parameters are taken as $\epsilon = 2.0$ (that of hexanes), $R_0 = 1.1$ (for saturated hydrocarbon spacer[26]), and the distance-dependence of λ_m is small and therefore neglected.[14,16]

The voltage-sensitive dyes based on electron transfer proposed herein are significantly different from those "charge-shift" dyes[7,10,27,28] based on electrochromism or the Stark-shift mechanism[29] despite some superficial similarities between them. For both the electron-transfer dyes and the "charge-shift" dyes, the distances of electron transfer or "charge-shift" need to be large for the dyes to achieve high voltage sensitivity. In the electrochromism case, electric fields shift the energy of the absorption and fluorescence spectra, leading to considerable field effect only near the edges of the spectra.[10] As a result, only a small portion of emitted photons are useful for voltage detection. In addition, a large charge-shift distance to increase voltage sensitivity at the same time leads to diminishing transition dipole moment and therefore low absorption cross section and fluorescence quantum yield.[30] In the electron-transfer case, electric fields vary the overall intensity of the fluorescence, making all the emitted photons useful for voltage detection. Because the electronic transition responsible for fluorescence is decoupled from the voltage-sensing electron-transfer process, it yields a better compromise between field sensitivity and fluorescence quantum yield (Figure 3b). This allows the fluorescence probes to have large voltage sensitivity, high fluorescence quantum yield, and fast time response and therefore may offer exciting opportunities in multisite imaging of neuronal activity with submillisecond time resolution, submicrometer spatial resolution, and large signal-to-noise ratios.

The electron-transfer mechanism in principle is applicable to all chromophores and therefore allows for great flexibility in the design of the electron-transfer-based dyes. On one hand, the fluorescence emitters can be chosen with optimal parameters for specific purposes such as one- or two-photon absorption cross section, fluorescence quantum yield, fluorescence lifetime, emission wavelength, photostability, and phototoxicity, etc., without sacrificing the electric-field response. On the other hand, because it is not photoexcited, the nonemitter in the donor−acceptor pair need only satisfy the preferred free energy change and electron-transfer rate. Candidates of particular interest for the emitters are derivatives of perylenetetracarboxdiimides[31−33] and fluorescent proteins.[1,34−36] Well-known for their remarkable photostability, large absorption cross section, and often near-unity fluorescence quantum yield, perylene dyes with low HOMO levels are good electron acceptors when paired with many chromophores.[26,37−39] In addition, limited live cell studies show they may also have low toxicity.[40] Fluorescent proteins, on the other hand, can be genetically coded with high cell specificity[1,34−36] and are therefore preferred in some cases over synthetic optical probes. The electron-transfer process can be introduced to modulate the fluorescence intensity of the proteins through introducing either a chromophore to form an electron-transfer pair with them[41,42] or an electron-transfer pair to form a FRET pair with the fluorescent proteins following known hybrid approaches.[43,44]

Acknowledgment. I thank Dr. Jeff Magee, Dr. Na Ji, and Dr. Rex Kerr at Janelia Farm Research Campus for helpful discussions. This work is supported by a startup fund from Indiana University.

References

(1) Knopfel, T.; Diez-Garcia, J.; Akemann, W. *Trends Neurosci.* **2006**, *29*, 160.
(2) Davila, H. V.; Salzberg, B. M.; Cohen, L. B.; Waggoner, A. S. *Nature (London) New Biol.* **1973**, *241*, 159.
(3) Conti, F. *Ann. Rev. Biophys. Bioeng.* **1975**, *4*, 287.
(4) Grinvald, A.; Frostig, R. D.; Lieke, E.; Hildesheim, R. *Physiol. Rev.* **1988**, *68*, 1285.
(5) Grinvald, A. *Annu. Rev. Neurosci.* **1985**, *8*, 263.
(6) Waggoner, A. S.; Grinvald, A. *Ann. N. Y. Acad. Sci.* **1977**, *303*, 217.
(7) Kuhn, B.; Fromherz, P.; Denk, W. *Biophys. J.* **2004**, *87*, 631.
(8) Waggoner, A. S. *Annu. Rev. Biophys. Bioeng.* **1979**, *8*, 47.
(9) Loew, L. M. *J. Biochem. Biophys. Methods* **1982**, *6*, 243.
(10) Kuhn, B.; Fromherz, P. *J. Phys. Chem. B* **2003**, *107*, 7903.
(11) Bixon, M.; Jortner, J. *J. Phys. Chem.* **1988**, *92*, 7148.
(12) Franzen, S.; Lao, K. Q.; Boxer, S. G. *Chem. Phys. Lett.* **1992**, *197*, 380.
(13) Tanaka, S.; Marcus, R. A. *J. Phys. Chem. B* **1997**, *101*, 5031.
(14) Marcus, R. A. *J. Chem. Phys.* **1965**, *43*, 679.
(15) Jortner, J. *J. Chem. Phys.* **1976**, *64*, 4860.
(16) Marcus, R. A. *Angew. Chem., Int. Ed. Engl.* **1993**, *32*, 1111.
(17) Nicholls, J. G.; Martin, A. R.; Wallace, B. G.; Fuchs, P. A. *From Neuron to Brain*, 4th ed.; Sinauer Associates, Inc.: Sunderland, MA, 2001.
(18) Tien, H. T.; Diana, A. L. *Chem. Phys. Lipids* **1968**, *2*, 55.
(19) Vos, M. H.; Vangorkom, H. J. *Biophys. J.* **1990**, *58*, 1547.
(20) Lockhart, D. J.; Boxer, S. G. *Chem. Phys. Lett.* **1988**, *144*, 243.
(21) Hilczer, M.; Tachiya, M. *J. Chem. Phys.* **2002**, *117*, 1759.
(22) Bulychev, A. A.; Niyazova, M. M.; Turovetsky, V. B. *Biochim. Biophys. Acta* **1986**, *850*, 218.
(23) Turro, N. J., *Modern Molecular Photochemistry*; University Science Books: Sausalito, CA, 1991.
(24) Wasielewski, M. R. *Chem. Rev.* **1992**, *92*, 435.
(25) Rehm, D.; Weller, A. *Isr. J. Chem.* **1970**, *8*, 259.
(26) Wasielewski, M. R. *J. Org. Chem.* **2006**, *71*, 5051.
(27) Loew, L. M.; Bonneville, G. W.; Surow, J. *Biochemistry* **1978**, *17*, 4065.
(28) Loew, L. M.; Simpson, L. L. *Biophys. J.* **1981**, *34*, 353.
(29) Liptay, W. *Angew. Chem., Int. Ed. Engl.* **1969**, *8*, 177.
(30) Grinvald, A.; Hildesheim, R.; Farber, I. C.; Anglister, L. *Biophys. J.* **1982**, *39*, 301.
(31) Langhals, H. *Heterocycles* **1995**, *40*, 477.
(32) Herrmann, A.; Mullen, K. *Chem. Lett.* **2006**, *35*, 978.
(33) Wurthner, F. *Chem. Commun.* **2004**, 1564.
(34) Tsien, R. Y. *Annu. Rev. Biochem.* **1998**, *67*, 509.
(35) Zimmer, M. *Chem. Rev.* **2002**, *102*, 759.
(36) Miyawaki, A. *Curr. Opin. Neurobiol.* **2003**, *13*, 591.
(37) Schmidt-Mende, L.; Fechtenkotter, A.; Mullen, K.; Moons, E.; Friend, R. H.; MacKenzie, J. D. *Science* **2001**, *293*, 1119.
(38) Wurthner, F.; Chen, Z. J.; Hoeben, F. J. M.; Osswald, P.; You, C. C.; Jonkheijm, P.; von Herrikhuyzen, J.; Schenning, A.; van der Schoot, P.; Meijer, E. W.; Beckers, E. H. A.; Meskers, S. C. J.; Janssen, R. A. J. *J. Am. Chem. Soc.* **2004**, *126*, 10611.
(39) Kaletas, B. K.; Dobrawa, R.; Sautter, A.; Wurthner, F.; Zimine, M.; De Cola, L.; Williams, R. M. *J. Phys. Chem. A* **2004**, *108*, 1900.

(40) Weil, T.; Abdalla, M. A.; Jatzke, C.; Hengstler, J.; Mullen, K. *Biomacromolecules* **2005**, *6*, 68.
(41) van Thor, J. J.; Gensch, T.; Hellingwerf, K. J.; Johnson, L. N. *Nat. Struct. Biol.* **2002**, *9*, 37.
(42) Choi, J. W.; Fujihira, M. *Appl. Phys. Lett.* **2004**, *84*, 2187.
(43) Gonzalez, J. E.; Tsien, R. Y. *Biophys. J.* **1995**, *69*, 1272.
(44) Chanda, B.; Blunck, R.; Faria, L. C.; Schweizer, F. E.; Mody, I.; Bezanilla, F. *Nat. Neurosci.* **2005**, *8*, 1619.

NL071163P